Scientia Iranica C (2022) 29(3), 1351–1363

Sharif University of Technology
Scientia Iranica
Transactions C: Chemistry and Chemical Engineering
http://scientiairanica.sharif.edu

Alkali activated cedar wood as an efficient adsorbent for Pb^{2+} removal from aqueous solutions: Optimization, kinetic, and thermodynamic study

M.A. Rahmatnia, A. Nouralishahi*, M. Bahaeddini, and A. Hallajisani

Energy, Environment, and Nanostructure Material Research Lab, Caspian Faculty of Engineering, College of Engineering, University of Tehran, Iran.

Received 2 April 2020; received in revised form 7 March 2021; accepted 24 May 2021

KEYWORDS
Cedar wood;
Adsorption isotherm;
Activated carbon;
Pb^{2+} removal.

Abstract. In the present study, the activated carbon prepared from cedar wood was synthesized via NaOH activation and optimized to be used as the adsorbent for Pb^{2+} removal from aqueous solutions in a batch process mode. The physicochemical properties of the synthesized adsorbent were examined by Scanning Electron Microscope (SEM), Fourier Transform Infrared Spectroscopy (FTIR), and Brunauer-Emmett-Teller (BET) analysis. In order to determine the optimum operational conditions, the effects of different parameters including pH, adsorbent dosage, contact time, temperature, and initial Pb^{2+} concentration on the adsorptive performance of synthesized samples were also investigated. According to the obtained results, the highest Pb^{2+} ion adsorption capacity (971.9 mg/g) took place in the optimum operational condition of pH = 4, adsorbent dosage of 0.025 g/L, contact time of 60 minutes, 300 ppm of Pb^{2+}, and 30°C. The results showed that among Langmuir, Freundlich, and Temkin isotherms, the obtained data fitted the best with the Freundlich model. Additionally, the process of Pb^{2+} adsorption was consistent with the pseudo-second order kinetics model, indicating that the rate-determining step is the surface adsorption that involves chemisorption. Finally, according to the calculated thermodynamic parameters, i.e., ΔH°, ΔS° & ΔG°, Pb^{2+} adsorption on activated cedar wood can be considered as an exothermic and spontaneous process.

1. Introduction

Lack of water resources is considered as one of the most important threats to human societies and sustainable development because of its significance to economic and population growth [1]. Water shortage problem may be the most important and complicated problem in the dry and semi-arid regions of the world. Throughout history, policymakers in these areas have been trying to solve the problem of water scarcity in different ways. Water pollution is one of the important environmental problems that can be caused by heavy metals. Heavy metals are produced by human activities such as industrial and mining operations and also, population increase and urbanization are non-biodegradable in nature, even at low concentrations [2,3]. Among different heavy metal ions, Pb^{2+} is one of the most major heavy metals which is commonly useful in many industries like battery manufacturing, smelting, paints, and paper industries [4–6]. However,

*. *Corresponding author. Tel.: +98 1344286461; Fax: +98 1344608600*
E-mail addresses: rahmatnia89@ ut.ac.ir (M.A. Rahmatnia); Nouralishahi@ut.ac.ir (A. Nouralishahi); mohsenbahaoddini@gmail.com (M. Bahaeddini); Hallaj@ut.ac.ir (A. Hallajisani)

doi: 10.24200/sci.2021.55733.4379

Pb^{2+} may cause many damages to human health like anemia, irritability, dizziness, and renal sickness [7] due to its toxicity, accumulation in food, and persistence in nature [8]. It can cause severe harms to human organs like kidney, liver, brain, etc. World Health Organization has determined the allowable concentration of Pb^{2+} (0.05 mg/L) in drinking water. There are lots of methods for removing Pb^{2+} ions from aqueous solutions such as chemical precipitation/coagulation, membrane technology, electrolytic reduction, ion exchange, and adsorption that had already been investigated [9,10]. However, high operational cost, unaffordability for large-scale metals, and ineffectiveness at higher concentrations make most of these methods inefficient. Adsorptive processes have been considered one of the most common approaches in energy and environment industries because of their easy operation and low cost [11–14]. Various low-cost materials such as biomass, moss, fly ash, natural materials like clay and zeolite, clinoptilolite, and synthetic resins have been tested as the adsorbent materials for removal heavy metals from water samples [14–22]. Among all, activated carbons are considered the most suitable materials for heavy metal removal from wastewater [23–32].

In the current study, the activated carbon from cedar wood has been synthesized to be used as the adsorbent in Pb^{2+} removal from water samples. The synthesis parameters including impregnation ratio (NaOH/precursor), activation temperature, and activation time are optimized. Also, the effects of operational parameters such as contact time, pH, temperature, and adsorbent dosage on the adsorption capacity of the optimized adsorbent are studied. In order to describe the adsorption mechanism, Langmuir, Freundlich, and Temkin isotherms are examined and the kinetic data are modeled by adsorption kinetic models (pseudo-first-order, pseudo-second-order, and intraparticle diffusion models).

2. Materials and methods

2.1. Preparation of the adsorbent

Cedar wood was collected from Khuzestan province, Iran. The samples were completely crushed and sieved to the mesh size of 150 (less than 0.1 mm in diameter), washed with distilled water, and then dried in an oven at 50°C for 2 h. Next, the carbonization process was carried out in a tube furnace under a nitrogen atmosphere at 500°C for 2 h and a heating rate of 20°C/min. After that, the sample was mixed with NaOH/Char ratio of 2:1 and stirred for 2 h. The resulting sample was dried in an oven at 80°C for 12 h. Then, the treated mixture was heated up to 575°C for 90 min at a heating rate of 20°C/min. All heating steps were carried out under a nitrogen stream. In order to remove the impurities, the sample was washed in 1 M HCl aqueous solution and then, neutralized with distilled water. In order to optimize the synthesis conditions, the same process as above was repeated in different conditions.

2.2. Characterization of the adsorbent

The morphology of the adsorbent surface was studied using a Scanning Electron Microscope (SEM, *JSM - 6700 F* model, made in *Japan*) analysis. In order to identify the surface functional groups, Fourier Transform Infrared Spectroscopy (FTIR) analysis was conducted. Also, Brunauer-Emmett-Teller (BET) surface area, pore diameters, and pore size distribution according to BET MP-method were estimated using N_2 adsorption/desorption at the boiling point of nitrogen. For this purpose, a TriStar II 3020 instrument (Micromeritics Co. USA) was employed.

2.3. Determination of point of zero charge (pH_{pzc})

The point at which the electrical charge density on the adsorbent surface is zero is called the isoelectric point (pH_{pzc}). It is important to specify this point in order to determine the adsorptive surface properties such that increasing pH resulted in an increased negative surface charge; therefore, positive ions can be easily adsorbed, and vice versa [33]. This experiment was conducted to determine the best range of pHs for the adsorption process. At first, 20 mL of 0.01 M NaCl solution was set at pH value (pH_i) of 2, 0.01 g of absorbent was added and it remained intact for 72 h. Then, the final pH value (pH_f) of the solution was measured by a pH meter (HI8915 HANNA, made in USA). This test was repeated at different pH values from 3 to 11. By plotting $pH_f - pH_i$ versus pH_i, the cross point of the curve with the horizontal axe represents the pH_{pzc} of activated carbon samples.

2.4. Effect of operational conditions

To examine the effect of operational parameters (i.e., pH, temperature, and adsorbent dosage) on the performance of activated carbon, 100 mL of $Pb(NO_3)_2$ solution (100 ppm) was poured in 500 mL beaker and the pH was adjusted at a certain value. Then, 0.025 g of adsorbent powder was added to the solution under vigorous stirring and at a controlled temperature. After equilibrium time, the adsorbent was filtered and separated from the solution. Then, 5 mL of each sample was tested to determine the concentration of Pb^{2+} by atomic adsorption apparatus.

2.5. Adsorption studies

The adsorption capacity of activated carbon samples and the removal efficiency of the Pb^{2+} were calculated using Eqs. (1) and (2), respectively:

$$q_e = \frac{c_0 - c_e}{m} \times V, \tag{1}$$

$$\%\text{Removal efficiency} = \frac{C_0 - C_e}{C_0} \times 100. \quad (2)$$

Here, C_0 and C_e are the initial and equilibrium concentrations of Pb^{2+} (mg/L), respectively, V is solution volume (L), and m is the adsorbent mass (g).

The adsorption kinetics of Pb^{2+} were assessed using the adsorption models of pseudo-first-order, pseudo-second-order, and intraparticle diffusion. Furthermore, different adsorption isotherm models including Langmuir, Freundlich, Temkin, and Dubinin-Radushkevich were employed to describe the adsorption equilibrium. Thermodynamic parameters of Pb^{2+} adsorption were calculated using Van't Hoff equation.

3. Results and discussions

3.1. Textural characterization of the adsorbent

Scanning Electron Microscope (SEM) is often used to examine the morphological features and adsorbent pore shapes [34]. The morphology and structure of the synthesized sample after adsorption of Pb^{2+} ions is shown in Figure 1. The SEM image revealed a highly porous structure of the adsorbent. The porosity and surface area characteristics of the adsorbent were estimated by BET method (see Table 1). The BET surface area and micropore area were found to be 2125 and 1989 m^2/g, respectively. The N_2 adsorption/desorption isotherms and the pore size distribution diagram of the sample are shown in Figure 2(a) and (b). The lack of hysteresis in N_2 adsorption/desorption isotherms suggests that the synthesized adsorbent has a microporous structure, which is also along with pore size distribution observed in Figure 2(b). According to Table 1, more than 85% of total pore volume belongs to pores with a diameter lower than 2 nm and this strongly confirms the results in Figure 2. Besides physical properties including the surface area and pore shape parameters, some chemical specifications such as surface functional groups affect adsorption capabilities of activated carbon. FTIR spectra (Figure 3) demonstrate the functional groups

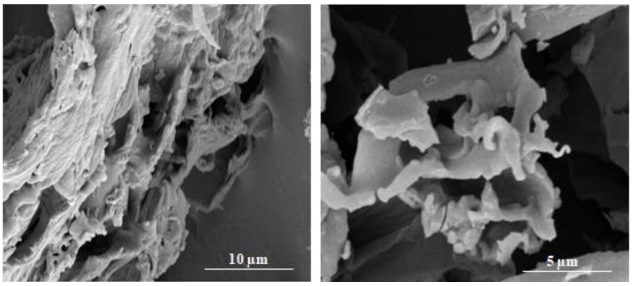

Figure 1. SEM photographs of the synthesized activated carbon at different resolutions.

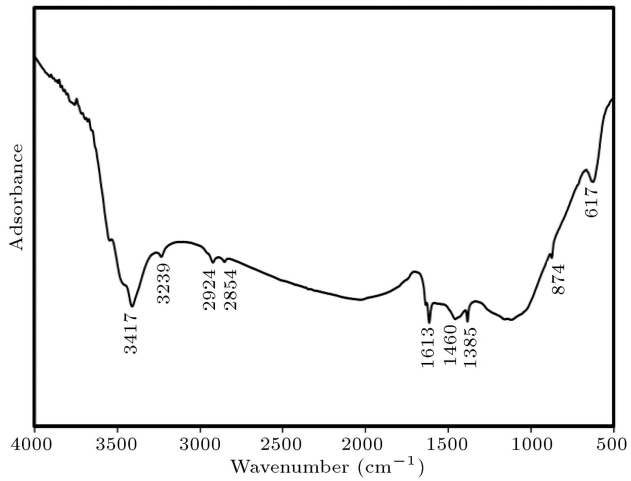

Figure 3. FTIR spectrum of the synthesized activated carbon.

Table 1. Characteristics of the synthesized activated carbon.

S_{BET} (m^2 g^{-1})	Micropore area (m^2 g^{-1})	External surface area (m^2 g^{-1})	Total pore volume (cm^3 g^{-1})	Micropore volume (cm^3 g^{-1})	Average pore diameter (nm)
2125	1989	136.8	0.91	0.78	1.71

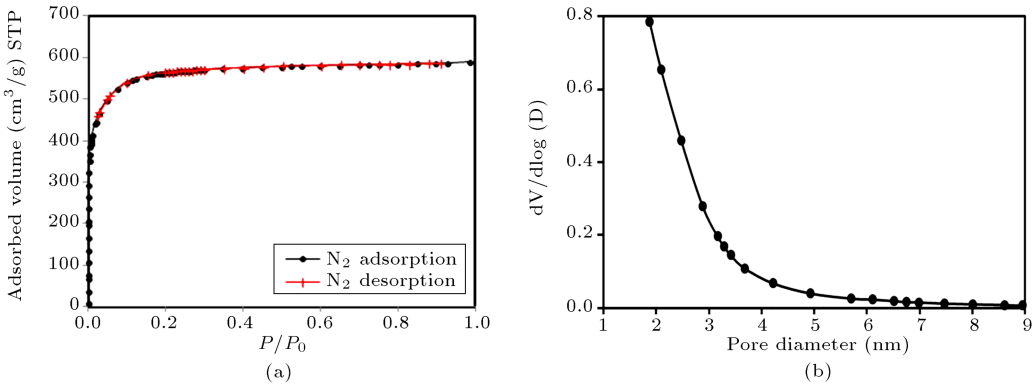

Figure 2. (a) N_2 adsorption/desorption isotherms. (b) Pore size distribution diagram of the synthesized activated carbon.

responsible for the adsorption of heavy metal ions (Pb^{2+}) on the nanostructured activated carbon. A peak around 1631 cm^{-1} can be ascribed to C=C and C=O stretching vibrations of anhydride, lactonic, or carboxyl groups [35–39]. An adsorption band located at 3471 cm^{-1} is assigned to O-H stretching vibration of hydrogen-bonded hydroxyl groups or adsorbed water [40–42]. The band at 1385 cm^{-1} can be attributed to C-H bending vibration of alkanes. These data prove the presence of some oxygen-containing groups on the surface, which may act as the adsorption sites on the surface of activated carbons interacting with Pb^{2+} ions.

3.2. The effect of synthesis parameters

3.2.1. Impregnation ratio

The ratio of the chemical activation agent, i.e., NaOH, to the carbonized material (impregnation ratio) has a profound influence on the final structure of activated carbons. Figure 4 shows changes in adsorption capacity with different impregnation ratios. The results revealed that the adsorption capacity increased continuously with the increasing NaOH/Char ratio until reaching a maximum at an impregnation ratio of 4:1. Nevertheless, above this ratio, the adsorption ratio declines slightly due possibly to the pores widening and the reduction in the specific surface area [27]. Also, at ratios lower than the maximum, the adsorption capacity is not high enough due to the lack of porosity [43].

3.2.2. Activation temperature

Figure 5 shows the effect of activation temperature on the Pb^{2+} adsorption capacity of the synthesized activated carbon. As can be seen here, the highest

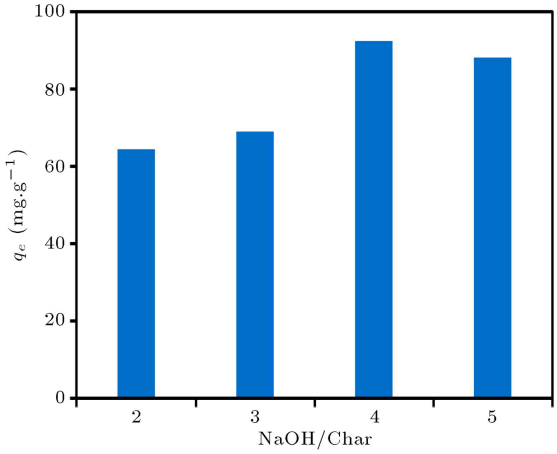

Figure 4. The effect of impregnation ratio on the adsorption capacity of Pb^{2+} on the synthesized activated carbons. The samples were prepared at activation temperature = 900°C and activation time of 90 min. The adsorption measurements were conducted at adsorbent dosage = 0.001 $g_{adsorbent}$/100 ml, Pb^{2+} concentration = 100 ppm, and temperature = 20°C.

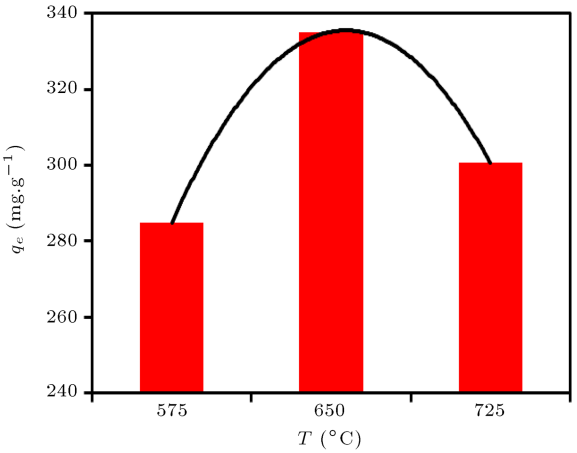

Figure 5. The effect of activation temperature on the adsorption capacity of Pb^{2+} on the synthesized activated carbons. The samples were prepared at activation time of 90 min and impregnation ratio of 4:1. The adsorption measurements were conducted at adsorbent dosage = 0.001 $g_{adsorbent}$/100 ml, Pb^{2+} concentration = 100 ppm, and temperature = 20°C.

adsorption capacity happens at 650°C. In fact, such a high carbonization temperature causes a large amount of non-carbonaceous species to be eliminated from the solid structure from the cellulosic source, i.e., walnut shell powder. This can deeply improve the porosity and final sorption capacity [44]. While at temperatures higher than the optimum (i.e., 650°C), the rate of oxidation reactions between surface carbon atoms and NaOH is too high, which may cause micro-pores to be converted into meso/macro-pores with a smaller surface area and lower adsorption capacity [45]. At lower temperatures, the adsorption capacity is not abundant due to the slow rate of oxidation reactions.

3.2.3. Activation time

During the synthesis procedure, the activation time (t_{act}) is an important parameter affecting final adsorption capacity of activated carbons. Figure 6 represents the effect of activation time on the performance of activated carbons in Pb^{2+} removal from water samples. According to the results presented here, the adsorption capacity reached 454 mg/g at the optimum tact of 60 min. So, according to the results in Figure 6, it seems that the activated carbon synthesized at t_{act} = 1 h, T_{act} = 650 K, and impregnation ratio of 4:1 exhibits better performance in Pb^{2+} removal from water, compared to the samples synthesized in other conditions. However, the final performance of the adsorbents is still deeply dependent on the operational conditions in which Pb^{2+} ion is adsorbed.

3.3. The effect of operational conditions

3.3.1. Determination of point of zero charge (pH_{pzc})

The results of the pH_{pzc} experiment are presented in Figure 7(a). According to the pH_f-pH_i values

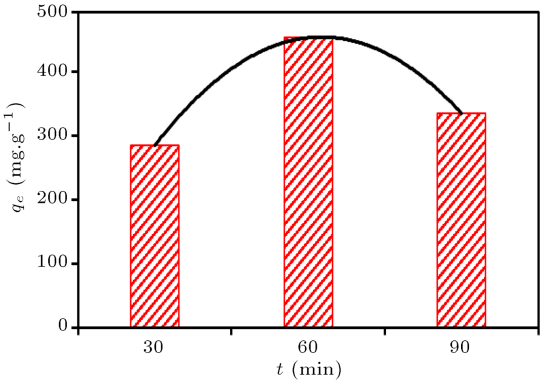

Figure 6. The effect of activation time on the adsorption capacity of Pb^{2+} on the synthesized activated carbons. The samples were prepared at activation temperature of 650°C and impregnation ratio of 4:1. The adsorption measurements were conducted at adsorbent dosage = 0.001 $g_{adsorbent}$/100 ml, Pb^{2+} concentration = 100 ppm, and temperature = 20°C.

reported in this figure, pH_{pzc} is likely to be at pH 4, which is very close to the pH_{pzc} value reported by Hafshejani et al. on carbonized cedar leaf, i.e., 3.76 [39]. At pH higher than pH_{pzc} = 4, the surface of the synthesized activated carbon is negatively charged, which is preferable for the adsorption of metal cations, i.e., Pb^{2+}, than anionic species [46,47]. However, the condition is more favorable for the adsorption of anionic groups at pH values lower than pH_{pzc}, where the surface of the adsorbent is covered by positively charged species.

3.3.2. Effect of pH

The pH of the solution is one of the most critical factors in adsorption processes because it could affect the solubility of metal ions, the degree of ionization of ion species during the reaction, the electrostatic bonding of ions to the relevant functional groups, and the number of metal ions on the functional groups of the adsorbent surface [33,48]. Figure 7(b) shows the effect of pH on the adsorption of Pb^{2+} by the adsorbent. Results demonstrate that in the range of pHs lower than 3, the adsorption capacity is lower due to the high concentrations of hydronium ions that compete with Pb^{2+} ions to adsorb onto the adsorbent surface. The adsorption capacity intensively increases following an increase in pH from 3 to 4. Although the Pb^{2+} removal increases at pH higher than 5, it seems that the higher removal performance results from the formation of precipitation of metal complexes at higher pH values rather than adsorption of Pb^{2+} ions. In fact, the adsorption of Pb^{2+} decreases at high pH values due to increase in the concentration of hydroxyl ions and the formation of the complex with the Pb^{2+} ions in the solution. As a result, in the range of pH values higher than 5, there is a strong possibility of precipitation [48]. Hence, the pH value of 4 is selected as the optimal point due to the reduction of positive surface charges and the increase in the negative charge density of the adsorbent [49].

3.3.3. Equilibrium time

The equilibrium contact time is the time required for the adsorption process to reach the equilibrium. To determine the equilibrium time for Pb^{2+} adsorption process, the adsorption capacity was measured during the time (Figure 8). According to the results, the equilibrium time was estimated to be 60 min when the adsorption data became steady during the time. In Figure 8, the adsorption capacity of the adsorbent is found to increase sharply with the contact time during the first 30 minutes, just before the adsorption capacity leveled off at its highest amount. Then, the rate of adsorption declines gradually until the equilibrium is reached. The fast adsorption rate at the beginning of the experiment may be explained by the large difference between the chemical potential of the vacant active sites on the surface and that in the bulk of the solution. This leads to a high driving force for mass transfer from

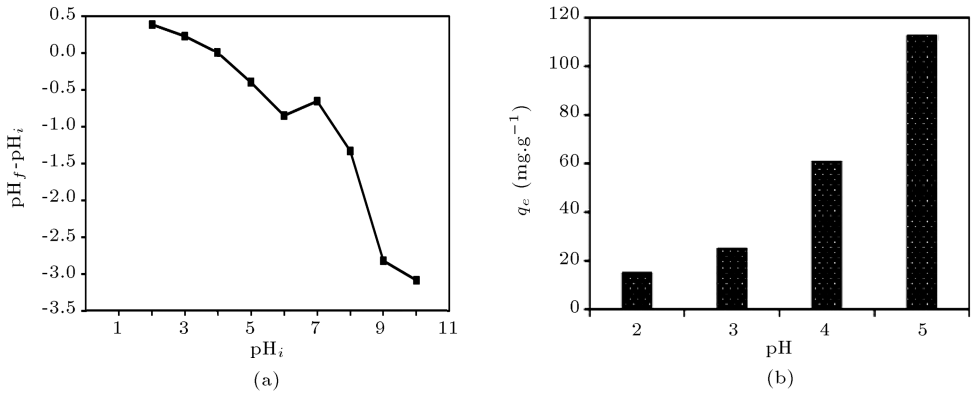

Figure 7. (a) pH_{pzc} of the activated carbon derived from cedar wood. (b) The effect of pH on the adsorption capacity of Pb^{2+} on the synthesized samples (adsorbent dosage = 0.1 $g_{adsorbent}$/100 ml, pH = 2, 3, 4, and 5; Pb^{2+} concentration = 100 ppm, and temperature = 20°C).

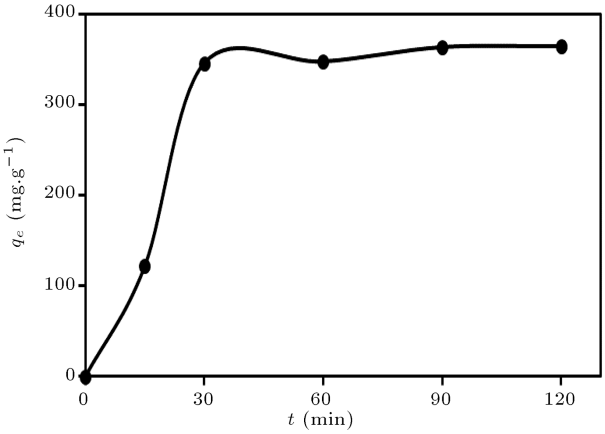

Figure 8. The effect of contact time on the adsorption capacity of Pb^{2+} on the synthesized activated carbons (adsorbent dosage = 0.025 $g_{adsorbent}$/100 ml, pH = 4, Pb^{2+} concentration = 100 ppm, and temperature = 20°C).

the bulk to the surface, thus increasing the absorption rate at the beginning [50,51].

3.3.4. Determination of optimum amount of adsorbent

Adsorbent dosage is essential to estimating the amount of adsorbent required for complete removal of a certain amount of metal ions from the solution [52]. In order to obtain the optimum adsorbent dosage of synthesized activated carbons, the adsorption capacities of Pb^{2+} at different dosages of adsorbent are depicted in Figure 9. The experiments were performed at different adsorbent concentrations from 0.025 to 0.1 g and the initial Pb^{2+} concentration of 100 mg/L. All data were recorded at 25°C and the optimum pH of 5.

The results in Figure 9 reveal that the maximum adsorption is related to the lowest initial amount of adsorbent with no optimum point, i.e., 0.025 g. According to the results, it is found that the adsorption capacity decreases with increase in the adsorbent

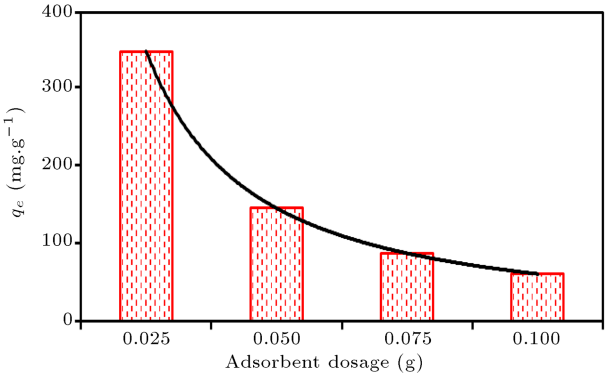

Figure 9. The effect of adsorbent dosage on the adsorption capacity of Pb^{2+} on the synthesized activated carbons (adsorbent dosage = 0.025, 0.05, 0.075, 0.1 $g_{adsorbent}$/100 ml, pH = 4, Pb^{2+} concentration = 100 ppm, and temperature = 20°C).

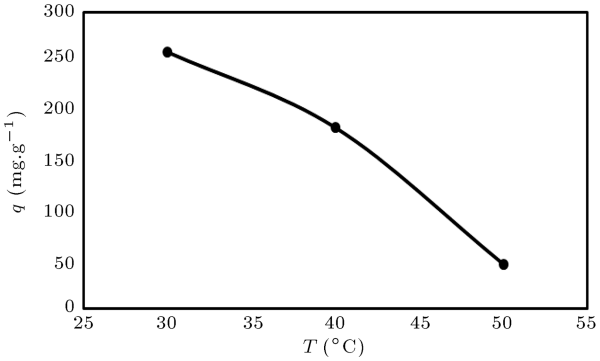

Figure 10. The effect of temperature on the adsorption capacity of Pb^{2+} on the synthesized activated carbons (adsorbent dosage = 0.025 $g_{adsorbent}$/100 ml, pH = 4, Pb^{2+} concentration = 100 ppm, and temperature = 30, 40, 50°C).

dose. It appears normal that the adsorption capacity increases with increasing adsorbent dosage as more adsorption sites are available. However, the reason usually presented to explain the negative effect of increasing the adsorbent dose is that when the amount of activated carbon in the solution increases, activated carbon beads begin to accumulate and form large clusters, thus reducing the available contact surface and resulting in a decrease in the amount of adsorbed ion [53].

3.3.5. Effect of temperature

Temperature is an environmental parameter that significantly affects the adsorption capacity of heavy metals. Figure 10 represents the adsorption capacity of Pb^{2+} at different temperatures. According to the results reported here, the adsorption capacity declined from 362.9 mg/g to 234.0 mg/g when the temperature increased from 30 to 50°C, indicating that the adsorption of Pb^{2+} on the synthesized activated carbon is an exothermic process. Therefore, lowering the temperature over the adsorption process of lead is thermodynamically desirable. In fact, the physical bonds between adsorbed species and surface-active sites might weaken at higher temperatures, leading to the lower adsorption capacity [33,54,55].

3.3.6. Effect of initial concentration of metal ion

Figure 11 shows the adsorption capacity of Pb^{2+} ions as a function of initial concentration of adsorbate. According to this figure, Pb^{2+} heavy metal uptake rises from 28.13 to 971.96 mg/g by increasing the initial concentration of Pb^{2+} ions from 25 to 300 mg/L. This can be attributed to the fact that a higher initial metal ion concentration not only provides a noticeable driving force to overcome the mass transfer resistance of the Pb^{2+} ions between the bulk and solid surface but also increases the number of collisions between metal ions and adsorbent, enhancing the overall adsorption capacity [56].

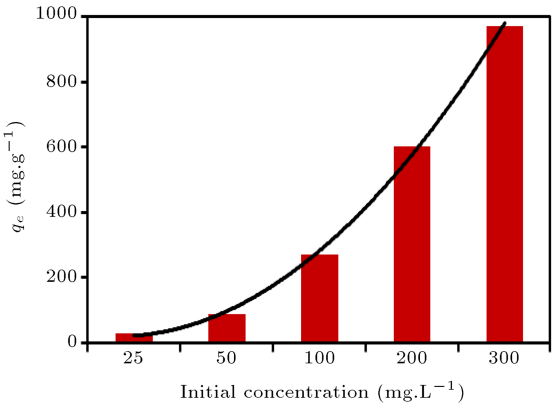

Figure 11. The effect of initial concentration of Pb^{2+} ion on the adsorption capacity of Pb^{2+} on the synthesized activated carbons (adsorbent dosage = 0.025 $g_{adsorbent}$/100 ml, pH = 4, Pb^{2+} concentration= 25, 50, 100, 200, 300 ppm, and temperature = 30°C).

3.4. Kinetics and equilibrium studies

3.4.1. Adsorption kinetics

In order to determine the kinetic parameters of adsorption, different adsorption isotherms, i.e., pseudo-first-order model (Eq. (3)), pseudo-second-order model (Eq. (4)), and intraparticle diffusion model (Eq. (5)) were examined. The related equations are shown as follows [55,57]:

$$\log(q_e - q_t) = \log(q_e) - \frac{k_1}{2.303}t, \tag{3}$$

$$\frac{t}{q_t} = \frac{t}{q_e} + \frac{1}{k_2 q_e^2}, \tag{4}$$

$$q_t = k_{id}t^{1/2} + C, \tag{5}$$

where q_t (mg/g) and q_e (mg/g) are the adsorption capacity of activated carbon at arbitrary time, t (min), and at equilibrium time, respectively. k_1 (1/min), k_2 (g/mg min), and k_{id} (mg/g min$^{1/2}$) are the adsorption rate constants of pseudo-first-order equation, pseudo-second-order equation, and intra-particle diffusion equation, correspondingly. C (mg/g) is the intra-particle diffusion constant, i.e., intercept of the line.

The diagrams for each kinetic model were plotted (Figure 12) and the results are tabulated in Table 2. By comparing the linear correlation coefficient (R^2) with the normal standard deviation ($\Delta\delta^2$) of applied models, the pseudo-second-order model with $R^2 > 0.90$ and the minimum standard deviation show the best fit with empirical data. This is in good compliance with what was reported in the literature for adsorption of Pb^{2+} on different adsorbents [3,32,38,39]. The

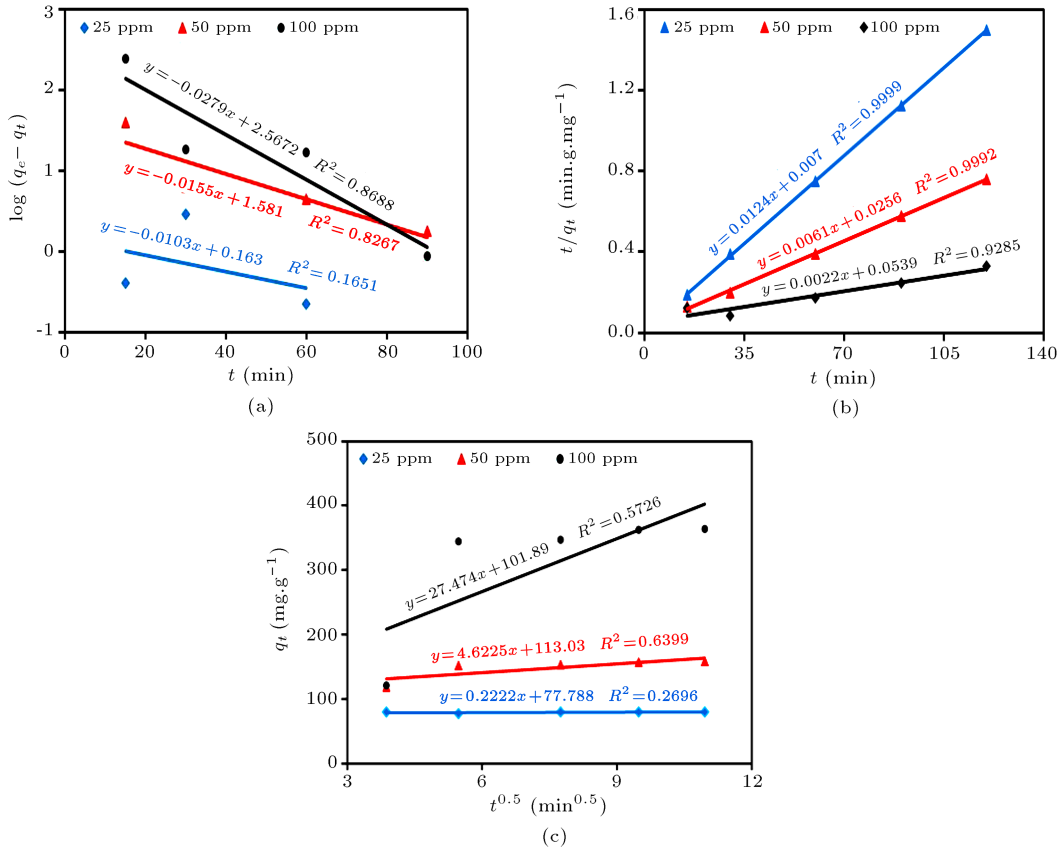

Figure 12. Kinetic models for adsorption of Pb^{2+} on the synthesized activated carbons: (a) Pseudo-first-order model, (b) pseudo-second-order model, and (c) intra-particle diffusion model.

Table 2. Parameters of kinetic models for the adsorption of Pb^{2+} on the synthesized activated carbon.

Pseudo-first-order model				
C (mg L^{-1})	K_1(min^{-1})	q_e (mg g^{-1})	$\%\Delta\delta^2$	R^2
25	0.0237	1.177	212	0.1651
50	0.0356	4.859	247	0.826
100	0.0642	13.029	339	0.8688
K_1: The model adsorption rate constant		$\Delta\delta^2$: Normal standard deviation		
q_e: The adsorption capacity at equilibrium		R^2: The linear correlation coefficient (R^2)		
Pseudo-second-order model				
C (mg L^{-1})	K_2 (min^{-1})	q_e (mg g^{-1})	$\%\Delta\delta^2$	R^2
25	0.01971	80.6	0.034	0.999
50	0.00145	163.9	7.09	0.999
100	0.000089	454.5	40	0.928
K_2: The model adsorption rate constant		$\Delta\delta^2$: Normal standard deviation		
q_e: The adsorption capacity at equilibrium		R^2: The linear correlation coefficient (R^2)		
Intraparticle diffusion model				
C (mg L^{-1})	K_{id} (g mg^{-1} $min^{-0.5}$)	C_{id} (mg g^{-1})	$\%\Delta\delta^2$	R^2
25	0.222	77.78	2.3	0.2696
50	4.625	113.03	13.3	0.6399
100	27.47	101.89	59	0.5726
K_{id}: The model adsorption rate constant		$\Delta\delta^2$: Normal standard deviation		
C_{id}: Intra-particle diffusion constant		R^2: The linear correlation coefficient (R^2)		

pseudo-second-order model assumes the following: a) monolayer adsorption; b) the same adsorption energy for each adsorbent and independent of surface coverage; c) adsorption occurring only at localized sites without any interactions between adsorbed pollutants; and d) the rate of adsorption being almost negligible compared to the initial adsorption rate [55]. The consistency between the pseudo-second-order model and experimental data in this study indicates that the rate-determining step is the surface adsorption that involves chemisorption [58].

3.4.2. Adsorption isotherms

Equilibrium relationships between the amount of Pb^{2+} ions adsorbed on the samples and their concentration remained in the solution at a constant temperature, which can be described by adsorption isotherms. In this study, three extensively equilibrium adsorption isotherms, namely the Langmuir, Freundlich, and Temkin model, were employed to analyze the experimental equilibrium data obtained for the adsorption of Pb^{2+} ions onto the adsorbent (Figure 13). Also, the parameters of each model are summarized in Table 3.

The linear form of theoretical Langmuir isotherm is given as (Eq. (6)):

$$\frac{\mathbf{1}}{q_e} = \frac{\mathbf{1}}{q_m K_L C_e} + \frac{\mathbf{1}}{q_m}, \tag{6}$$

where q_m (mg/g) is the monolayer adsorption capacity and K_L is Langmuir equilibrium constant (1/mg). Both of the above are calculated by plotting $1/q_e$ versus $1/C_e$ (Figure 13(a)). To evaluate the Langmuir isotherm, a separation factor (R_L) (Eq. (7)) is defined as follows:

$$R_L = \frac{1}{1 + K_L C_0}, \tag{7}$$

where C_0 is the highest initial solute concentration. The nature of the adsorption process is indicated by the value of the separation factor, i.e., the process can be irreversible ($R_L = 0$), unfavorable ($R_L > 0$), favorable ($0 < R_L < 1$), or linear ($R_L = 1$) [59]. Considering the value of $R_L = 0.021$ shown in Table 3 confirms the favorable adsorption of Pb^{2+} ions on the prepared samples.

The empirical Freundlich isotherm assumes the non-ideal sorption on heterogeneous surfaces [60] and its linear form equation (Eq. (8)) is expressed as below:

$$lnq_e = lnK_F + \frac{1}{n} lnC_e, \tag{8}$$

where K_F (g^{-1}) is Freundlich constant and $1/n$ is the heterogeneity factor, both of which are determined by plotting $\ln(q_e)$ against $\ln(C_e)$ (Figure 13(b)). As the value of heterogeneity factor is below unity ($1/n$ =

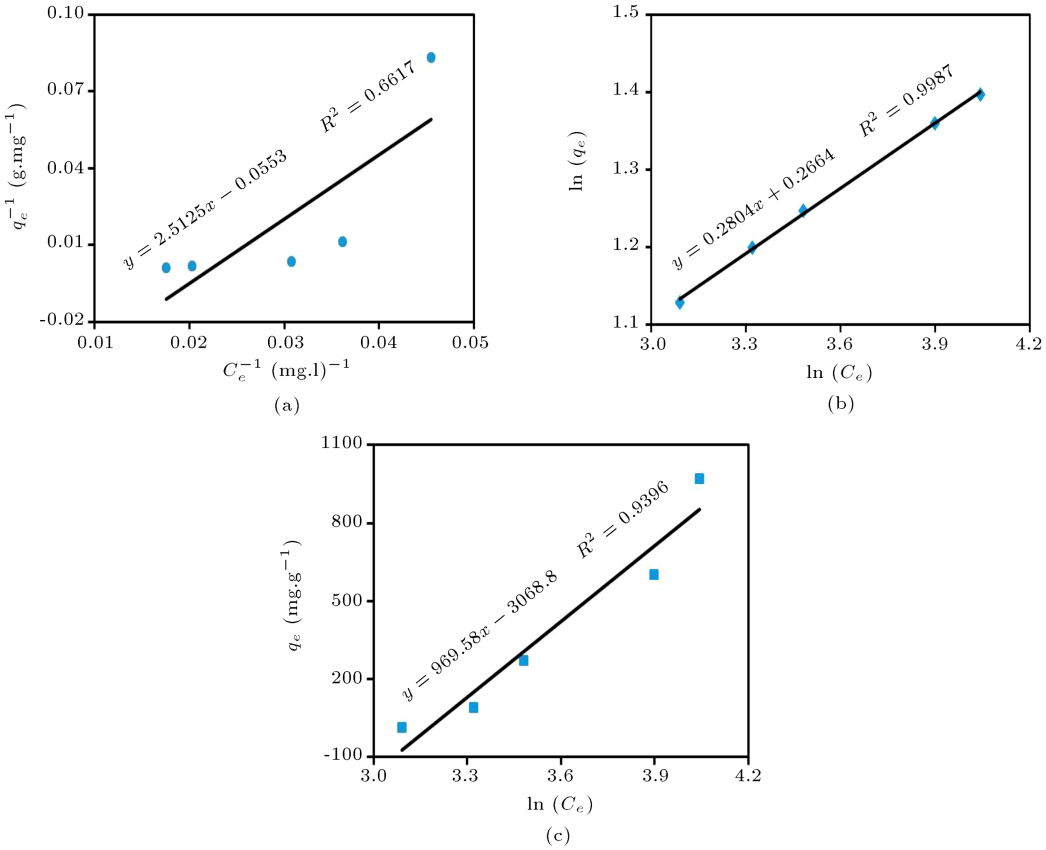

Figure 13. Adsorption isotherm models for adsorption of Pb^{2+} on the synthesized activated carbons: (a) Langmuir, (b) Freundlich, and (c) Temkin.

Table 3. Parameters of isotherm models used for the adsorption of Pb^{2+} of the synthesized activated carbon.

Langmuir		**Freundlich**		**Temkin**	
K_L (L mg^{-1})	7.197	K_f (L mg^{-1})	1.305	b	0.0088
q_m (mg g^{-1})	18.08	n	3.563	A_T (L g^{-1})	0.989
R_L	0.021	$1/n$	0.281	R^2	0.939
R^2	0.6617	R^2	0.998	–	–

0.281), the adsorption process type is inferred from chemisorption [61].

Temkin and Pyzhev represented the following equation (Eq. (9)), presuming that heat of adsorption of the molecules on the layer would decline linearly with coverage due to the adsorbate/adsorbent interactions and ignoring very low and very large values of concentration:

$$q_e = BlnA_T + BlnC_e, \qquad B = \frac{RT}{b}, \tag{9}$$

where A_T and B are the Temkin constants.

By comparing the linear correlation coefficient (R^2) of the summarized data in Table 3, it appears that the Freundlich isotherm model provides the best fit with the empirical data for the adsorption of Pb^{2+} ions ($R^2 = 0.998$).

3.4.3. Determination of thermodynamic parameters

The thermodynamic parameters namely standard free energy (ΔG°), standard enthalpy change (ΔH°), and standard entropy change (ΔS°) can describe the nature of adsorption. The standard enthalpy (ΔH°) and entropy (ΔS°) were calculated through the following Van't Hoff equation (Eq. (10)):

$$\ln\left(\frac{q_e}{C_e}\right) = \frac{\Delta S^\circ}{R} - \frac{\Delta H^\circ}{RT}, \tag{10}$$

where R is the universal gas constant and T is temperature in Kelvin. The Van't Hoff plot of Pb^{2+} ions adsorption onto the synthesized adsorbent is represented in Figure 14. The Gibbs free energy was obtained from the equation below (Eq. (11)):

$$\Delta G^\circ = \Delta H^\circ + \Delta S^\circ. \tag{11}$$

Table 4. Thermodynamic parameters of Pb^{2+} adsorption of the synthesized activated carbon.

T (K)	ΔG° (kJ mol^{-1})	ΔH° (kJ mol^{-1})	ΔS° (kJ mol^{-1} K^{-1})
303	−90.64	−199.72	−0.36
313	−87.04	–	–
323	−83.44	–	–

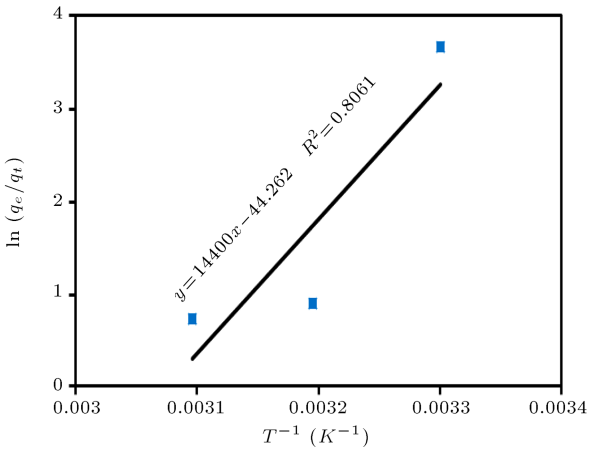

Figure 14. The Van't Hoff plot of Pb^{2+} adsorption on the synthesized activated carbon.

The calculated thermodynamic parameters are listed in Table 4. The negative enthalpy (ΔH°) value of -119.72 (kJ mol^{-1}) indicates that the interactions between Pb^{2+} ions and the adsorbent are exothermic. The entropy was found negative too, suggesting that the Pb^{2+} ions adsorption was a reversible process. Also, the negative values of Gibbs free energy indicate the favorable thermodynamics and spontaneous nature of the process. The increase in ΔG° values from -90.64 to -83.44 (kJ mol^{-1}) with the temperature suggests the feasibility of the Pb^{2+} removal at lower temperatures, preferable for industrial applications.

4. Conclusion

In the current survey, the activated carbon obtained from cedar tree was synthesized using NaOH to be applied as a new and efficient adsorbent for Pb^{2+} heavy metal ions. In order to study the morphology, surface species, and micropore structure of the synthesized activated carbon, Scanning Electron Microscope (SEM), Fourier Transform Infrared Spectroscopy (FTIR), and Brunauer-Emmett-Teller (BET) analyses were conducted. The effects of different parameters such as pH, temperature, equilibrium time, and initial concentration of Pb^{2+} ions on final adsorption capacity were also investigated. The maximum adsorption of Pb^{2+} was 971.9 mg/g, which was achieved in the optimum condition of pH = 5, contact time of 60 minutes, adsorbent dosage of 0.025 g/L, temperature of 30°C, and metal ion concentration of 300 ppm. Among Langmuir, Freundlich, and Temkin isotherm models, the experimental data fitted the best with the Freundlich model. The process of Pb^{2+} ions adsorption was well simulated with the pseudo-second-order kinetics model, indicating that chemical adsorption was the dominant mechanism of adsorption. The negative thermodynamic parameters (ΔH°, ΔS° and ΔG°) confirmed that Pb^{2+} adsorption was an exothermic and spontaneous process. According to the results reported here, the nanostructured activated carbon from cedar wood can be considered as a promising adsorbent for Pb^{2+} ions and other heavy metals from aqueous solutions.

References

1. Gohari, A., Eslamian, S., Mirchi, A., et al. " Water transfer as a solution to water shortage: a fix that can backfire", *Journal of Hydrology*, **491**, pp. 23–39 (2013).
2. Demirbas, A. "Heavy metal adsorption onto agro-based waste materials: a review", *Journal of Hazardous Materials*, **157**(2–3), pp. 220–229 (2008).
3. Liang, S., Guo, X., and Tian, Q. "Adsorption of Pb^{2+} and Zn^{2+} from aqueous solutions by sulfured orange peel", *Desalination*, **275**(1–3), pp. 212–216 (2011).
4. Kohli, S.K., Handa, N., Bali, S., et al. "Current scenario of Pb toxicity in plants: unraveling plethora of physiological responses", *Reviews of Environmental Contamination and Toxicology*, **249**, pp. 153–197 (2019).
5. Jamil, M., Zia, M.S., and Qasim, M. "Contamination of agro-ecosystem and human health hazards from wastewater used for irrigation", *Journal of the Chemical Society of Pakistan*, **32**(3), pp. 370–378 (2010).
6. Khan, S., Cao, Q., Zheng, Y., et al. "Health risks of heavy metals in contaminated soils and food crops irrigated with wastewater in Beijing", *China. Environmental Pollution*, **152**(3), pp. 686–692 (2008).
7. Schwartz, J. "Costs and benefits of reducing lead in gasoline", Report published by US Environmental Agency (1984).
8. Moreno-Barbosa, J.J., López-Velandia, C., del Pilar Maldonado, A., et al. "Removal of lead (II) and zinc (II) ions from aqueous solutions by adsorption onto activated carbon synthesized from watermelon shell and walnut shell", *Adsorption*, **19**(2–4), pp. 675–685 (2013).

9. Kurniawan, T.A., Chan, G.Y., Lo, W.-H., et al. "Physico-chemical treatment techniques for wastewater laden with heavy metals", *Chemical Engineering Journal*, **118**(1–2), pp. 83–98 (2006).
10. Collivignarelli, M.C., Abbà, A., Bestetti, M., et al. "Electrolytic recovery of nickel and copper from acid pickling solutions used to treat metal surfaces", *Water, Air, & Soil Pollution*, **230**(5), pp. 1–13 (2019).
11. Nouralishahi, A., Bahaeddini, M., Mahinnezhad, Sh., et al. "Activated nanoporous carbon from walnut shell as a promising adsorbent for methane storage in ANG technology", *Scientia Iranica, C*, **26**(6), pp. 3447–3455 (2019).
12. Rashidi, A., Nouralishahi, A., Khodadadi, A., et al. "Nanoporous carbon as a promising novel methane adsorbent for adsorbed natural gas technology", *Journal of Natural Gas Chemistry*, **20**, pp. 664–668 (2011).
13. Rashidi, A., Nouralishahi, A., Khodadadi, A., et al. "Modification of single wall carbon nanotubes (SWNT) for hydrogen storage", *International Journal of Hydrogen Energy*, **35**, pp. 9489–9495 (2010).
14. Nguyen, T.C., Loganathan, P., Nguyen, T.V., et al. "Adsorptive removal of five heavy metals from water using blast furnace slag and fly ash", *Environmental Science and Pollution Research*, **25**, pp. 20430–20438 (2018).
15. Dash, S., Chaudhuri, H., Gupta, R., et al. "Adsorption study of modified coal fly ash with sulfonic acid as a potential adsorbent for the removal of toxic reactive dyes from aqueous solution: kinetics and thermodynamics", *Journal of Environmental Chemical Engineering*, **6**(5), pp. 5897–5905 (2018).
16. Vafajoo, L., Cheraghi, R., Dabbagh, R., et al. "Removal of cobalt (II) ions from aqueous solutions utilizing the pre-treated 2-Hypnea Valentiae algae: Equilibrium, thermodynamic, and dynamic studies", *Chemical Engineering Journal*, **331**, pp. 39–47 (2018).
17. Okoli, C.P., Diagboya, P.N., Anigbogu, I.O., et al. "Competitive biosorption of Pb (II) and Cd (II) ions from aqueous solutions using chemically modified moss biomass (Barbula lambarenensis)", *Environmental Earth Sciences*, **76**(1), pp. 33–42 (2017).
18. Jiménez-Castañeda, M.E., and Medina, D.I. "Use of surfactant-modified zeolites and clays for the removal of heavy metals from water", *Water*, **9**(4), pp. 235–246 (2017).
19. Qiu, Q., Jiang, X., Lv, G., et al. "Adsorption of heavy metal ions using zeolite materials of municipal solid waste incineration fly ash modified by microwave-assisted hydrothermal treatment", *Powder Technology*, **335**, pp. 156–163 (2018).
20. Radi, S., El Abiad, C., Moura, N., et al. "New hybrid adsorbent based on porphyrin functionalized silica for heavy metals removal: synthesis, characterization, isotherms, kinetics and thermodynamics studies", *Journal of Hazardous Materials*, **370**, pp. 80–90 (2019).
21. Oliveira, J.A., Cunha, F.A., and Ruotolo, L.A. "Synthesis of zeolite from sugarcane bagasse fly ash and its application as a low-cost adsorbent to remove heavy metals", *Journal of Cleaner Production*, **229**, pp. 956–963 (2019).
22. Kobayashi, Y., Ogata, F., Nakamura, T., et al. "Synthesis of novel zeolites produced from fly ash by hydrothermal treatment in alkaline solution and its evaluation as an adsorbent for heavy metal removal", *Journal of Environmental Chemical Engineering*, **8**(2), pp. 103687–103692 (2020).
23. Li, J., Xing, X., Li, J., et al. "Preparation of thiol-functionalized activated carbon from sewage sludge with coal blending for heavy metal removal from contaminated water", *Environmental Pollution*, **234**, pp. 677–683 (2018).
24. Niazi, L., Lashanizadegan, A., and Sharififard, H. "Chestnut oak shells activated carbon: Preparation, characterization and application for Cr (VI) removal from dilute aqueous solutions", *Journal of Cleaner Production*, **185**, pp. 554–561 (2018).
25. Gao, X., Wu, L., Xu, Q., et al. "Adsorption kinetics and mechanisms of copper ions on activated carbons derived from pinewood sawdust by fast H_3PO_4 activation", *Environmental Science and Pollution Research*, **25**(8), pp. 7907–7915 (2018).
26. Mahmood, T., Aslam, M., Naeem, A., et al. "Adsorption of as (iii) from aqueous solution onto iron impregnated used tea activated carbon: equilibrium, kinetic and thermodynamic study", *Journal of the Chilean Chemical Society*, **63**(1), pp. 3855–3866 (2018).
27. Nayak, A., Bhushan, B., Gupta, V., et al. "Chemically activated carbon from lignocellulosic wastes for heavy metal wastewater remediation: Effect of activation conditions", *Journal of Colloid and Interface Science*, **493**, pp. 228–240 (2017).
28. Naushad, M., Ahamad, T., Al-Maswari, B.M., et al. "Nickel ferrite bearing nitrogen-doped mesoporous carbon as efficient adsorbent for the removal of highly toxic metal ion from aqueous medium", *Chemical Engineering Journal*, **330**, pp. 1351–1360 (2017).
29. Rodiguez, M.H., Yperman, J., Carleer, R., et al. "Adsorption of Ni (II) on spent coffee and coffee husk based activated carbon", *Journal of Environmental Chemical Engineering*, **6**(1), pp. 1161–1170 (2018).
30. Song, M., Wei, Y., Cai, S., et al. "Study on adsorption properties and mechanism of Pb^{2+} with different carbon based adsorbents", *Science of the Total Environment*, **618**, pp. 1416–1422 (2018).
31. Asuquo, E., Martin, A., Nzerem, P., et al. "Adsorption of Cd (II) and Pb (II) ions from aqueous solutions using mesoporous activated carbon adsorbent: Equilibrium, kinetics and characterisation studies", *Journal of Environmental Chemical Engineering*, **5**(1), pp. 679–698 (2017).
32. El-Sayed, M. and Nada, A.A. "Polyethylenimine functionalized amorphous carbon fabricated from oil palm

leaves as a novel adsorbent for Cr (VI) and Pb (II) from aqueous solution", *Journal of Water Process Engineering*, **16**, pp. 296–308 (2017).

33. Tounsadi, H., Khalidi, A., Abdennouri, M., et al. "Biosorption potential of Diplotaxis harra and Glebionis coronaria L. biomasses for the removal of Cd (II) and Co (II) from aqueous solutions", *Journal of Environmental Chemical Engineering*, **3**(2), pp. 822–830 (2015).

34. Gao, Y., Yue, Q., Gao, B., et al. "Preparation of high surface area-activated carbon from lignin of papermaking black liquor by KOH activation for Ni (II) adsorption", *Chemical Engineering Journal*, **217**, pp. 345–353 (2013).

35. Azhagapillai, P., Al Shoaibi, A., and Chandrasekar, S. "Surface functionalization methodologies on activated carbons and their benzene adsorption", *Carbon Letters*, **31**(3), pp. 419–426 (2021).

36. Christou, C., Agapiou, A., and Kokkinofta, R. "Use of FTIR spectroscopy and chemometrics for the classification of carobs origin", *Journal of Advanced Research*, **10**, pp. 1–8 (2018).

37. Herrera-Kao, W.A., Loría-Bastarrachea, M.I., Pérez-Padilla, Y., et al. "Degradation of poly (caprolactone), poly (lactic acid), and poly (hydroxybutyrate) studied by TGA/FTIR and other analytical techniques", *Polymer Bulletin*, **75**(9), pp. 4191–4205 (2018).

38. Yu, J., Tong, M., Sun, X., et al. "A simple method to prepare poly (amic acid)-modified biomass for enhancement of lead and cadmium adsorption", *Biochemical Engineering Journal*, **33**(2), pp. 126–133 (2007)

39. Hafshejani, L.D., Nasab, S.B., Gholami, R.M., et al. "Removal of zinc and lead from aqueous solution by nanostructured cedar leaf ash as biosorbent", *Journal of Molecular Liquids*, **211**, pp. 448–456 (2015).

40. Nouralishahi, A., Rashidi, A.M., Mortazavi, Y., et al. "Enhanced methanol electro-oxidation reaction on Pt-CoOx/MWCNTs hybrid electro-catalyst", *Applied Surface Science*, **335**, pp. 55–64 (2015).

41. Nouralishahi, A., Mortazavi, Y., Khodadadi, A.A., et al. "Characteristics and performance of urea modified Pt-MWCNTs for electro-oxidation of methanol", *Applied Surface Science,* **467**, pp. 335–344 (2019).

42. Li, J., Zhang, P., Chen, L., et al. "Strong, tough and healable elastomer nanocomposites enabled by a hydrogen-bonded supramolecular network", *Composites Communications*, **22**, p. 100530 (2020).

43. Girgis, B.S., Yunis, S.S., and Soliman, A.M. "Characteristics of activated carbon from peanut hulls in relation to conditions of preparation", *Materials Letters*, **57**(1), pp. 164–172 (2002).

44. Lua, A.C. and Yang, T. "Effect of activation temperature on the textural and chemical properties of potassium hydroxide activated carbon prepared from pistachio-nut shell", *Journal of Colloid and Interface Science*, **274**(2), pp. 594–601 (2004).

45. Daud, W.M.A.W., Ali, W.S.W., and Sulaiman, M.Z. "The effects of carbonization temperature on pore development in palm-shell-based activated carbon", *Carbon*, **38**(14), pp. 1925–1932 (2000).

46. Borah, D. and Senapati, K. "Adsorption of Cd (II) from aqueous solution onto pyrite", *Fuel*, **85**(12–13), pp. 1929–1934 (2006).

47. Órfão, J., Silva, A., Pereira, J., et al. "Adsorption of a reactive dye on chemically modified activated carbons-influence of pH", *Journal of Colloid and Interface Science*, **296**(2), pp. 480–489 (2006).

48. Pang, Y., Zeng, G., Tang, L., et al. "PEI-grafted magnetic porous powder for highly effective adsorption of heavy metal ions", *Desalination* , **281**, pp. 278–284 (2011).

49. Naiya, T.K., Bhattacharya, A.K., and Das, S.K. "Clarified sludge (basic oxygen furnace sludge)-an adsorbent for removal of Pb (II) from aqueous solutions-kinetics, thermodynamics and desorption studies", *Journal of Hazardous Materials*, **170**(1), pp. 252–262 (2009).

50. Amarasinghe, B. and Williams, R. "Tea waste as a low cost adsorbent for the removal of Cu and Pb from wastewater", *Chemical Engineering Journal*, **132**(1–3), pp. 299–309 (2007).

51. Ünlü, N. and Ersoz, M. "Adsorption characteristics of heavy metal ions onto a low cost biopolymeric sorbent from aqueous solutions", *Journal of Hazardous Materials*, **136**(2), pp. 272–280 (2006).

52. Du, Y., Zhu, L., and Shan, G. "Removal of Cd^{2+} from contaminated water by nano-sized aragonite mollusk shell and the competition of coexisting metal ions", *Journal of Colloid and Interface Science*, **367**(1), pp. 378–382 (2012).

53. Brudey, T., Largitte, L., Jean-Marius, C., et al. "Adsorption of lead by chemically activated carbons from three lignocellulosic precursors", *Journal of Analytical and Applied Pyrolysis*, **120**, pp. 450–463 (2016).

54. Bazrafshan, E., Amirian, P., Mahvi, A., et al. "Application of adsorption process for phenolic compounds removal from aqueous environments: a systematic review", *Global NEST Journal*, **18**(1), pp. 146–163 (2016).

55. Abbas, S.H., Ismail, I.M., Mostafa, T.M., et al. "Biosorption of heavy metals: a review", *J. Chem. Sci, Technol*, **3**(4), pp. 74–102 (2014).

56. Hadi, P., Xu, M., Ning, C., et al. "A critical review on preparation, characterization and utilization

of sludge-derived activated carbons for wastewater treatment", *Chemical Engineering Journal*, **260**, pp. 895–906 (2015).

57. Abdelfattah, I., Ismail, A.A., Al Sayed, F., et al. "Biosorption of heavy metals ions in real industrial wastewater using peanut husk as efficient and cost effective adsorbent. Environmental Nanotechnology", *Monitoring & Management*, **6**, pp. 176–183 (2016).
58. Zhou, L., Yu, Q., Cui, Y., et al. "Adsorption properties of activated carbon from reed with a high adsorption capacity", *Ecological Engineering*, **102**, pp. 443–450 (2017).
59. Karagöz, S., Tay, T., Ucar, S., et al. "Activated carbons from waste biomass by sulfuric acid activation and their use on methylene blue adsorption", *Bioresource Technology*, **99**(14), pp. 6214–6222 (2008).
60. Ng, C., Losso, J.N., Marshall, W.E., et al. "Freundlich adsorption isotherms of agricultural by-product-based powdered activated carbons in a geosmin-water system", *Bioresource Technology*, **85**(2), pp. 131–135 (2002).
61. Gimbert, F., Morin-Crini, N., Renault, F., et al. "Adsorption isotherm models for dye removal by cationized starch-based material in a single component system: error analysis", *Journal of Hazardous Materials*, **157**(1), pp. 34–46 (2008).

Biographies

Mohammad Ali Rahmatnia received his BSc and MSc in Chemical Engineering from University of Tehran. His research area of interest is the adsorption process in energy and environmental applications.

Amiddedin Nouralishahi received his PhD in Nanotechnology-Chemical Engineering from University of Tehran. Currently, he is an Assistant Professor of Chemical Engineering at Caspian Faculty of Engineering, University of Tehran. His main research interests include the application of nanomaterials in chemical processes.

Mohsen Bahaeddini received his BSc in Chemical Engineering from University of Tehran in 2018. His main area of research is related to the preparation of nanomaterials for separation technologies.

Ahmad Hallajisani received his PhD in Chemical Engineering from University of Tehran. He is currently an Assistant Professor of Chemical Engineering at Caspian Faculty of Engineering, University of Tehran. His main research interests include adsorption and bioengineering.